Comparison of unidirectional and bidirectional airfoils in a tidal stream turbine

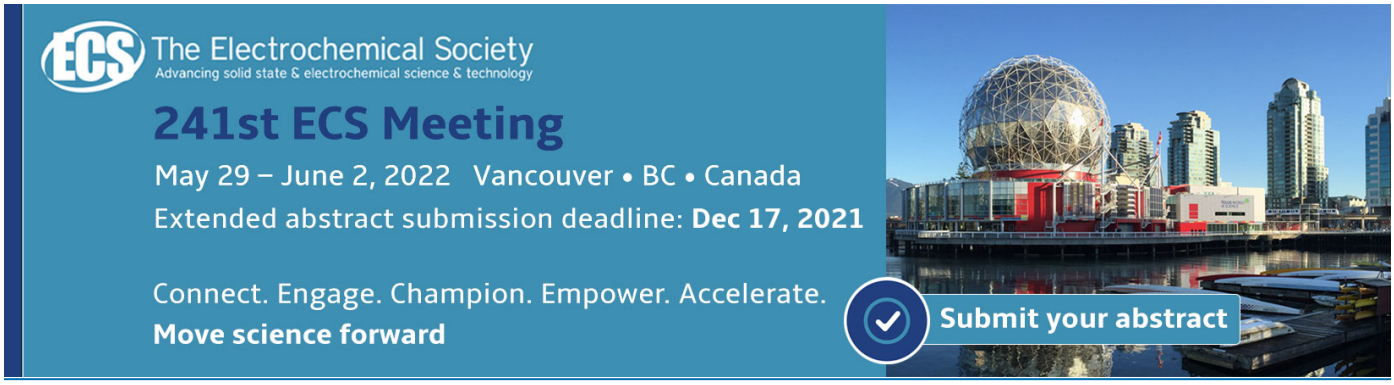

Comparison of unidirectional and bidirectional airfoils in a tidal stream turbine

K E T Giljarhus [1], J O Owolabi [1] and O A Frøynes [2]

[1] University of Stavanger, Stavanger, Norway
[2] Framo Innovation AS, Bergen, Norway

E-mail: knut.e.giljarhus@uis.no

Abstract. Tidal stream turbines offer an attractive method for stable renewable energy generation. Due to the periodicity of the tidal stream, a tidal stream turbine can be designed to operate in a bidirectional manner, thereby avoiding a yaw control system. This article compares a unidirectional design with a bidirectional design to estimate the expected power loss for the bidirectional design. First, a blade-element momentum theory approach is used to find optimum pitch angles for the blades and give a low-cost estimate of the power production. Next, fully-resolved computational fluid dynamics simulations are performed to validate the BEMT approach and gain insight into the flow patterns. The two approaches estimate that the power output of the bidirectional design is approximately 15-20 % lower than for the unidirectional design. This suggests that although a bidirectional design will have some power loss compared to a unidirectional design it is an interesting alternative as it can yield the same power output for both the ebb and the tide. The study also serves as a starting point for further optimization of the bidirectional design.

1. Introduction

With increased need for renewable energy, tidal stream turbines can be a viable addition to the energy production mix. The tidal stream is more predictable than wind giving more stable energy production and the higher density of water compared to air means higher energy production per surface area. The seawater is a harsh environment, which puts significant requirements on the engineering of a tidal stream turbine. This has been noted as a key reason why tidal energy is not currently commercially viable[1]. To keep maintenance to a minimum, the system should have as few moving parts as possible. One innovation in use in many tidal turbine designs today is the use of an open-centre turbine, which extracts energy through a direct-drive magnet generator in the rim of the turbine. This removes the need for a gearbox, making the system more reliable. The high solidity of an open-centre device also gives a more slowly rotating turbine, which reduces wear and is also beneficial for marine life. An additional element of tidal energy is that the flow is typically more stable, with only slight variations in direction. A horizontal-axis wind turbine will typically need a yaw gear to orient itself towards the wind. For a tidal turbine, due to the more predictable flow pattern, an attractive alternative is to make the turbine bidirectional so that power can be produced in both the ebb and flow phases of the tidal flow pattern.

The use of computational tools to estimate power output from a tidal stream turbine has been extensively studied in the scientific literature. Fleming and Wilden[2] used CFD simulations to investigate the influence of a duct to increase power output. The tidal turbine was represented

as an actuator disc, i.e. a sink in the momentum equations. Recently, blade-resolved CFD simulations are also becoming more common. Liu and Hu[3] and Ghassemi et al.[4] showed good agreement with experiments using blade-resolved simulations with a multiple-reference frame approach for the rotation of the turbine. The most general CFD methodology, with the most direct solution of the fundamental equations without any assumptions and simplifications is the use of blade-resolved simulations with a sliding mesh. This technique was used e.g. by Tampier et al.[5] to study a diffuser-augmented turbine design. Despite the increased use of detailed CFD simulations, simplified methods such as BEMT are also still in use. In [6], a BEMT method was used along with CFD simulations to study a duct-augmented tidal stream turbine. There are also methodologies combining these two methods. Belloni et al.[7] used a BEMT simulation to inject representative forces from the blades into the CFD simulation, instead of a direct representation of the blade geometry.

There has also been some studies investigating the difference in unidirectional and bidirectional designs. Li et al.[8] studied the efficiency of various blade curvatures in a bidirectional design. Nedyalkov and Wosnik[9] performed 2D simulations and experiments of lift and drag for various bidirectional airfoil shapes. In [10], experiments and simulations were performed for a low-solidity turbine, comparing a unidirectional and a bidirectional design.

In this work, we compare the potential power output of a high-solidity, horizontal axis tidal stream turbine using both cambered, unidirectional airfoils and elliptic, bidirectional airfoils. First, a BEMT solver is used to optimize the pitch and give an initial estimate of power output. Next, blade-resolved CFD simulations are performed to gain further insight into the flow patterns.

2. Materials and methods

2.1. Definitions

The rotational speed of the turbine is related to the speed of the tidal current through the tip speed ratio,

$$\mathrm{TSR} = \frac{\omega R}{V}, \tag{1}$$

where ω is the angular velocity of turbine, R is the radius of the turbine and V is the tidal stream velocity. The power is expressed as the power coefficient,

$$C_P = \frac{P}{\frac{1}{2}\rho A V^3} \tag{2}$$

Here, P is the power generated by the turbine, calculated by the torque on the turbine multiplied by its angular velocity. ρ is the fluid density and A the frontal area of the turbine.

2.2. Turbine design

The turbine design considered in this work is a 7-bladed, high-solidity turbine with open centre. The airfoil used for the unidirectional design is the NACA 65-415. For the bidirectional design, an elliptic airfoil with similar thickness as the NACA airfoil was chosen. A comparison of the two airfoils, as well as a 3D model of the turbine is shown in Figure 1.

2.3. Blade Element Momentum Theory

The blade element momentum theory combines blade element theory and momentum theory. In the blade element theory, the blade is divided into smaller sections that are assumed to operate independently of each other. The forces on each section can then be calculated using tabulated values for lift and drag for the specific airfoil shape for that section. In the momentum theory, the rotor is assumed to behave as a uniform momentum sink and expressions for the forces are derived using mass and momentum conservation. In both of these approaches, new

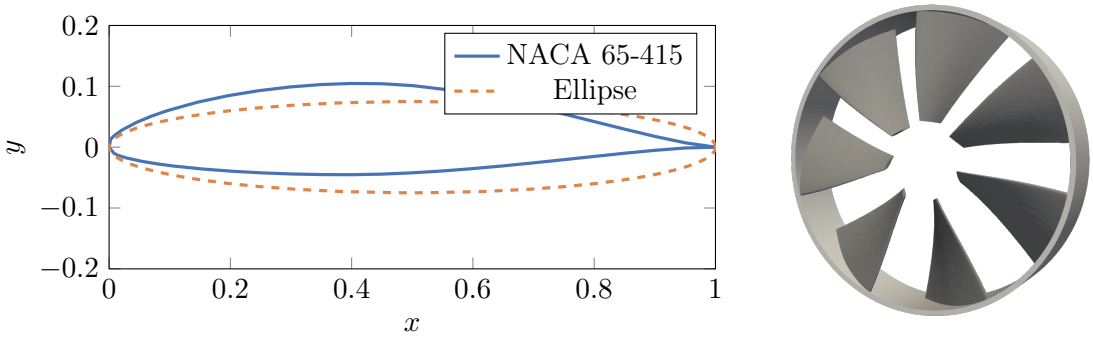

Figure 1: Comparison of unidirectional and bidirectional airfoil (left) and a 3D render of the full turbine geometry (right).

unknowns appear in the form of induction factors. The velocity that a blade section sees is not the actual incoming flow velocity in the axial direction or the angular velocity of the turbine in the tangential direction. The axial velocity is decreased due to the presence of the turbine and the angular velocity is increased due to swirl. Combining the blade element theory and the momentum theory allows a calculation of these induction factors.

In this work, we use the open-source software pyBEMT for the BEMT simulations[11]. This code also contains an optimization of the pitch angle using a genetic algorithm, more specifically the differential evolution algorithm[12]. As mentioned above, a BEMT simulation requires tabulated values for lift and drag for the selected blade profiles. Here, the values for the NACA airfoil is obtained from XFOIL, through the QBlade software[13]. For the elliptic airfoil, XFOIL does not converge due to limitations with the panel method. Hence, experimental values for an elliptic airfoil was used instead[14, 15].

2.4. Computational Fluid Dynamics

In computational fluid dynamics, the governing equations for fluid flow are solved numerically. This offers a generic way of tackling a wide variety of fluid flow problems. The fluid domain is divided into smaller cells and discrete approximations are introduced for the continuous terms of the equations. Also, due to the inherent complexity of turbulence, turbulence models are typically used.

The simulations in this work are performed in the open-source CFD simulation software OpenFOAM, version 7 [16, 17].

2.4.1. Numerical settings and turbulence model Simulations are performed with a Reynolds-averaged Navier-Stokes (RANS) turbulence model, more specifically the k-ω SST turbulence model [18]. The PIMPLE algorithm is used for pressure-velocity coupling. This algorithm couples the SIMPLE and PISO algorithms, and can allow for larger time steps in a stable manner compared to just applying the PISO algorithm. Here, the time advancement is set to one degree of rotation per time step, and the simulations are performed for eight full rotations of the turbine. For discretization, a first-order implicit Euler method is used for time discretization and second-order discretization schemes are used for spacial discretization. For the convective terms, a second-order central-upwind scheme with a Sweby limiter is used [19].

2.4.2. Computational domain and boundary conditions The size of the computational domain is $20D \times 10D \times 10D$, where D is the diameter of the turbine. This gives a blockage ratio lower than 3.0 %. The geometry is placed centrally in the domain, $5D$ from the inlet. The inlet boundary

is given a uniform constant velocity, with zero gradient for pressure. Medium turbulence levels are assumed, with a turbulent intensity of 5 %. The flow Reynolds number is 300 000, while the rotational Reynolds number varies between 150 000 and 375 000 depending on the tip speed ratio of the turbine.

At the outlet a fixed pressure is set with zero gradient for the remaining variables. The sides of the domain use a slip boundary condition. For the turbine, a no-slip boundary condition is applied and a wall function is used blending the fully-resolved region and the wall function region. The rotation of the geometry is handled using the Arbitrary Mesh Interface (AMI) method.

2.4.3. Computational mesh `snappyHexMesh`, a hex-dominated unstructured mesh generator that is part of OpenFOAM, is used to generate the mesh. The grid is refined using refinement boxes around the turbine. Between seven and nine levels of 2:1 refinement is applied towards the turbine giving a cell size of 2 mm close to the blades. Additionally, prism layers with an expansion ration of 1.2 between each layer were inserted near the blades to resolve the thin boundary layer in this region. The average non-dimensional distance to the first grid cell is often used as a measure of grid adequacy,

$$y^+ = \frac{u_\star y}{\nu}, \tag{3}$$

where $u_\star$ is the friction velocity and ν the kinematic viscosity of the fluid. In the simulations presented here, an average value of $y^+ \approx 2$ was found.

The total number of cells in the mesh is around 20 million. An overall view of the mesh, as well as a close-up of the surface mesh on the blade, is shown in Figure 2.

3. Results

3.1. Validation

Since no experimental data is available on an open-centre, high-solidity turbine, the experimental data from [20] for a three-bladed horizontal axis turbine is used to validate the computational methods. This experiment has been widely used for validation in other tidal stream turbine studies[3, 21, 6].

The results for the power coefficient are shown in Figure 3. The results for both the BEMT simulations and the CFD simulations are in reasonable agreement with the experimental results. In general, it should be easier to simulate the optimal point with fully-resolved CFD. At sub-optimal tip speed ratios, the flow behavior becomes more complex due to stall and flow separation. Even at the optimal operation point, there is some disagreement with the experiments for the CFD simulations. This could partly be attributed to the fact that the trailing edge of the blade was cut to make it more amenable for the meshing process. This is shown in Figure 4, which shows a line integral convolution plot of the velocity pattern at two cross sections along the blade for a tip speed ratio of TSR = 6. This figure also shows that near the root of the blade there is some flow separation near the trailing edge of the airfoil, while for the airfoil closer to the tip the flow remains attached along the blade. This flow pattern was also observed in other simulation studies of the same turbine[3].

3.2. Pitch optimization

The original pitch is set using the relative velocity found from just the inflow velocity and the angular velocity directly. The actual inflow velocity seen by the blade will be lower and the angular velocity higher, hence a lower pitch angle will give a more optimal flow over the blade. This is taken into account by the BEMT method used for the optimization.

Figure 5 shows the original pitch compared with the optimized pitch for the unidirectional design, as well as the power coefficient as a function of the tip speed ratio for the two cases. The optimized design has a lower pitch angle as expected. The optimized pitch angle gives a

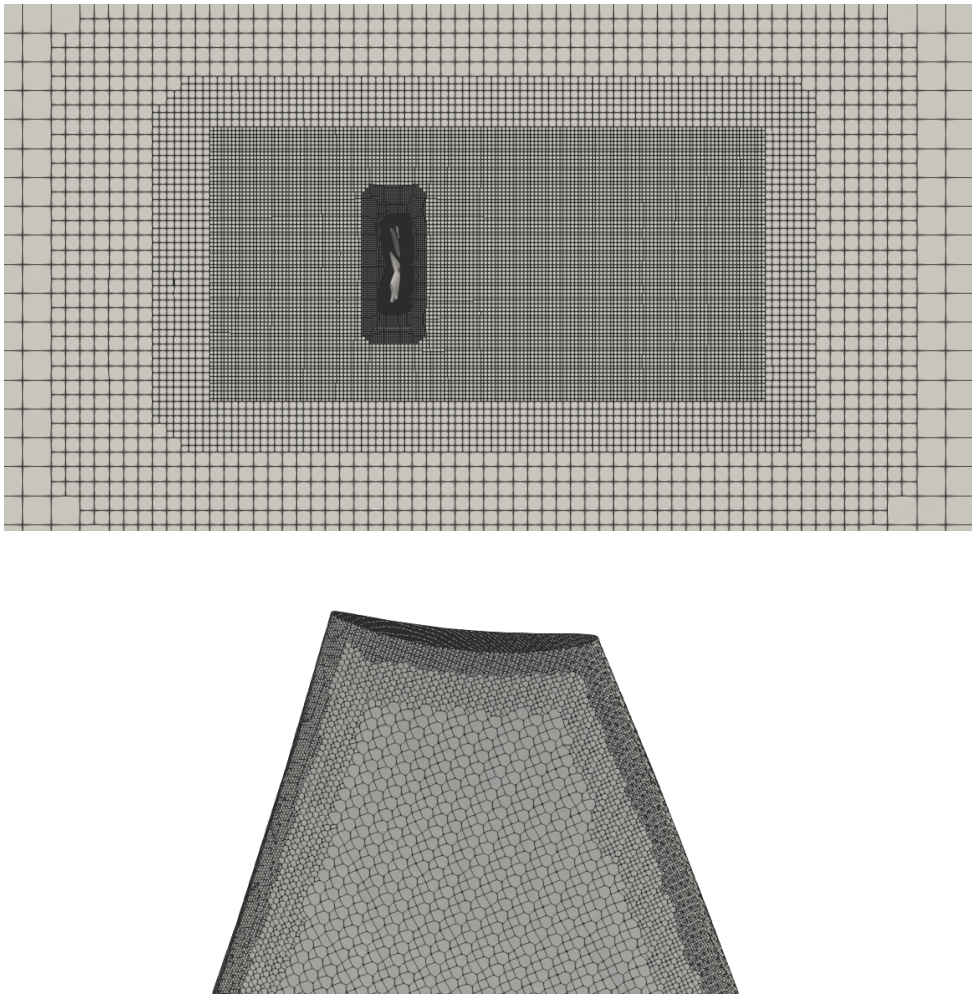

Figure 2: Overall layout of mesh (top) and close-up of mesh near blade (bottom).

simulated 27 % higher power at the optimal point. The optimal point is shifted towards a higher tip speed ratio, and the operational envelope is also slightly wider for the optimized design.

3.3. Comparison between blades with NACA profile and elliptic profile

Figure 6 shows the power coefficient as a function of tip speed ratio for the unidirectional and bidirectional design. Both the BEMT simulations and the CFD simulations are included in the figure. For the BEMT method, a difference of 22 % was found in peak power output. For the CFD method, a difference of 15 % was found. Both methods show a relatively narrow power coefficient curve, with the power coefficient rapidly tapering off from the optimal point. At a tip speed ratio 25 % higher or lower than the optimum, the power output is reduced by more than 50 %. This behavior was also seen in other studies of high-solidity turbines, e.g. [6]. This is in contrast to the validation example with a low-solidity turbine, where the difference is only 15 %.

Figure 7 shows a comparison of the flow pattern over the blades for the unidirectional and bidirectional design. Note that the elliptic airfoil has a higher pitch angle to compensate for the lack of camber to increase the lift. However, the lift produced by the elliptic airfoil is still lower than the airfoil with the NACA profile. For the elliptic profile, a large region of separated flow can be observed after the trailing edge of the airfoil. This is due to the blunt shape of the airfoil compared to the sharper edge of the NACA profile.

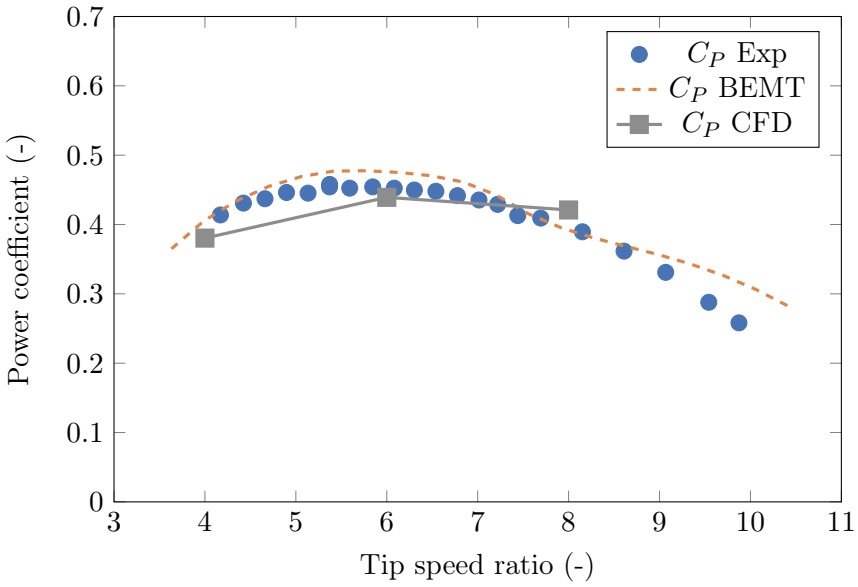

Figure 3: Comparison of power coefficient for the BEMT model and CFD model with the experimental results from [20].

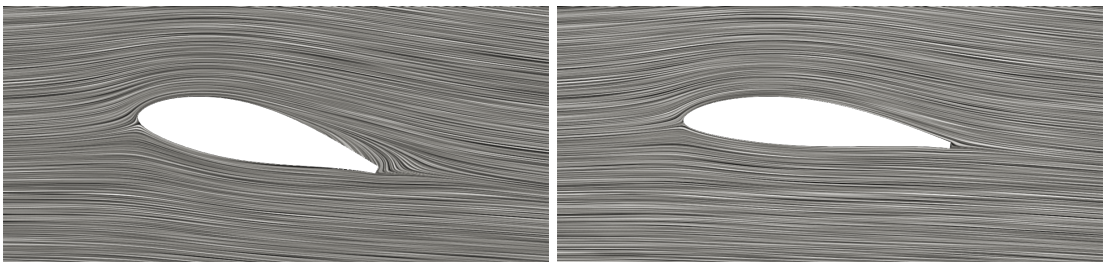

Figure 4: Examples of flow pattern from CFD simulation of the unidirectional profile. Line integral convolution plot of relative velocity over the blade at $r = 0.1D$ (left) and $r = 0.5D$ (right).

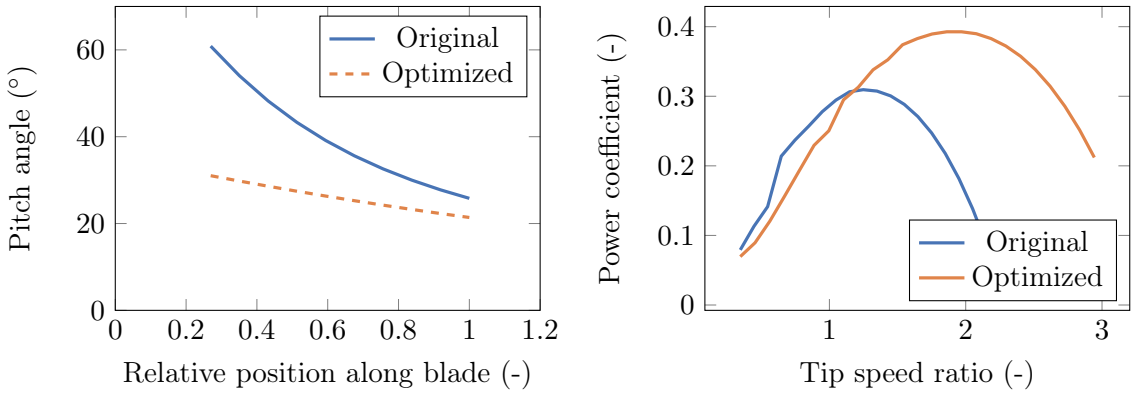

Figure 5: Comparison of pitch angles (left) and power coefficients (right) for the initial and optimized blades in the BEMT simulation.

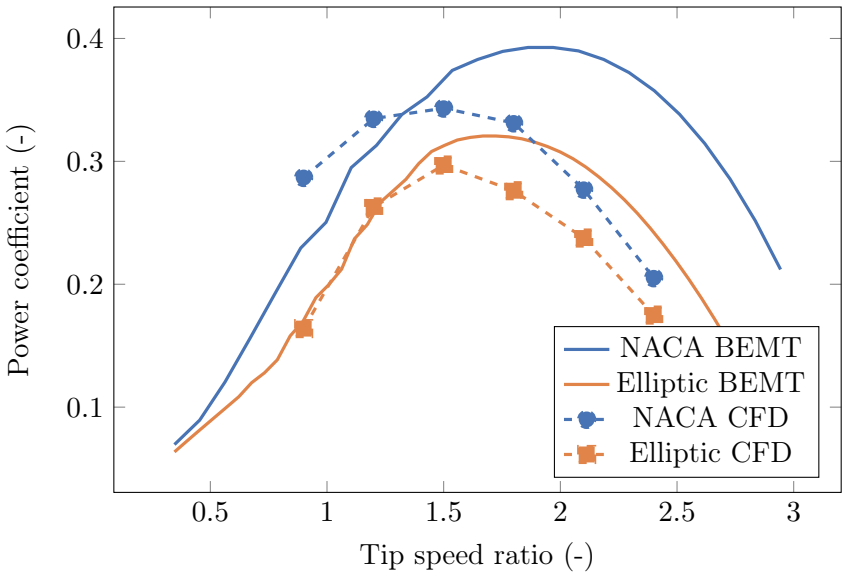

Figure 6: Comparison of power coefficients for the NACA profile and the elliptic profile for both the BEMT method and the CFD method.

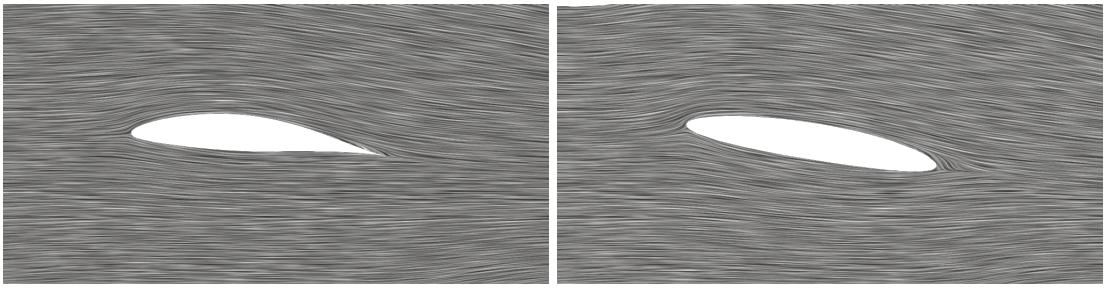

Figure 7: Line integral convolution plot of relative velocity over the high solidity turbine at $r = 0.36D$ for the NACA profile (left) and the elliptic profile (right).

4. Discussion and conclusion

This article investigated the difference in performance for an open centre, high-solidity tidal stream turbine when using a unidirectional or bidirectional blade design. The unidirectional design used a NACA 65-415 airfoil profile, while the bidirectional design used an elliptic airfoil profile. Two different simulation methods were used, a blade-element momentum theory approach and fully-resolved CFD approach. The two methods were shown to be in good agreement with experimental values for a low-solidity three-bladed turbine.

The bidirectional design gave a power coefficient of approximately 0.3. This indicates a 15-20 % difference between the bidirectional and unidirectional design. In [10], a bidirectional design was found to only have a 1.6 % difference compared to a unidirectional design. The discrepancy could be because they used symmetric foils also for the unidirectional design. Additionally, the turbine was a low-solidity, three-bladed turbine which is different from the turbine considered here.

The CFD method in general gave a lower power output than the BEMT method, and the peak was found at a lower tip speed ratio. This could have multiple explanations. First of all, the BEMT method contains correlations for the losses at the tip and hub of the blade. While these have some physical interpretation, they are designed for thinner blades. For the turbine

considered here, the outer rim could have higher losses than what is included in the correlation. At the tip of the blade, there is also an acceleration of the flow due to the open centre, which could also lead to higher losses. Further investigation into the modification of the BEMT approach for a high-solidity turbine is an interesting topic for future work.

Only a single airfoil profile was used for the blade in this work. There could be performance gains to be had with selecting different profiles along the blade. Additionally, other airfoil shapes than the one considered here or an optimization of the airfoil shape could be considered. The same is also the case for the elliptic airfoil shape, and work on optimizing this shape is currently being undertaken by the authors. The shape of the outer rim could also be optimized, and a duct could be added for additional performance gains.

Finally, only computational methods were used in this work. Although these were compared to experimental data from the literature for a three-bladed design, experimental data on a high-solidity design would be useful for further validation of the numerical models.

Acknowledgments

We acknowledge Roar Kristensen from Norwegian Tidal Solutions and Martin Sigmundstad from Validé for technical discussions and support related to this work.

References

[1] Rourke F O, Boyle F and Reynolds A 2010 *Appl energy* **87** 398–409
[2] Fleming C F and Willden R H 2016 *International Journal of Marine Energy* **16** 162–173
[3] Liu C and Hu C 2015 Numerical prediction of the hydrodynamic performance of a horizontal tidal turbines *Int Conf OMAE* vol 56598
[4] Ghassemi H, Ghafari H and Homayoun E 2018 *Sci J Maritime Uni Szczecin* **55**
[5] Tampier G, Troncoso C and Zilic F 2017 *Ocean Eng* **145** 138–147
[6] Borg M G, Xiao Q, Allsop S, Incecik A and Peyrard C 2020 *Renew Energy*
[7] Belloni C, Willden R and Houlsby G 2017 *Renew Energy* **108** 622–634
[8] Li L, Chen Y and Wang Z 2013 Numerical calculations of bidirectional characteristics on tidal current runner *IMECE*
[9] Nedyalkov I and Wosnik M 2014 Performance of bi-directional blades for tidal current turbines *FEDSM* (ASME)
[10] Guo B, Wang D, Zhou X, Shi W and Jing F 2020 *Water* **12** 22
[11] Giljarhus K E T 2020 *J Open Source Softw* **5** 2480
[12] Storn R and Price K 1997 *J Global Optim* **11** 341–359
[13] Marten D, Wendler J, Pechlivanoglou G, Nayeri C and Paschereit C 2013 *Int J Emerg Technol Adv Eng* **3** 264–269
[14] Choi S and Kwon O J 2008 *J Aircraft* **45** 641–650
[15] Kwon K and Park S O 2005 *J Aircraft* **42** 1642–1644
[16] Weller H G, Tabor G, Jasak H and Fureby C 1998 *Comput Phys* **12** 620–631
[17] Jasak H, Jemcov A, Tukovic Z *et al.* 2007 OpenFOAM: A C++ library for complex physics simulations *CMND* vol 1000 (IUC Dubrovnik Croatia)
[18] Menter F R, Kuntz M and Langtry R 2003 *Turb Heat Mass Transf* **4** 625–632
[19] Sweby P K 1984 *SIAM J Numer Ana* **21** 995–1011
[20] Bahaj A, Molland A, Chaplin J and Batten W 2007 *Renew energy* **32** 407–426
[21] Amiri H A, Shafaghat R, Alamian R, Taheri S M and Shadloo M S 2019 *Int J Numer Meth Heat & Fluid Flow*